

# Consideration on Stainless Steel Plate Plastic Deformed by Fluid Impact Substances and Pressured Nitrogen Blasting

ADRIAN ROSCA<sup>1</sup>, DANIELA ROSCA<sup>1</sup>, VASILE NASTASESCU<sup>2</sup>

1. University of Craiova

13, A. I. Cuza Street, 200585, Craiova

2. Ministry for Education and Research

ROMANIA

[adrosca2003@yahoo.com](mailto:adrosca2003@yahoo.com), <http://www.ucv.ro>, [vasile.nastasescu@mec.edu.ro](mailto:vasile.nastasescu@mec.edu.ro)

*Abstract:* The paper presents a plastic deformation method for thin plates made of stainless steel, plastic deformed by pressured nitrogen blasting combined with impact fluid substances. There are presented experimental results for comparative values of deformation velocities obtained by different initial pressured nitrogen blasting, respectively by pressured nitrogen blasting combined with several quantities of impact fluid substances.

*Key-Words:* - Pressured nitrogen blasting, Plastic deformation, Stainless steel thin plates

## 1. Introduction

In the present stage of technological development, a new method of metal plate plastic deformation process by shock waves gazes blasting, combined with impact substances (pulverulent / fluid), comes to complete, but not to replace, the diversity of high velocity deformation procedures: explosive substances, exploding wires in gasses, electro-hydraulic or magneto-hydraulic impulses, Dynapac hammer [1, 2, 3].

Designed for the first time in a Romanian R&D Institute, this new method was developed to produce parts for medium and low voltage special electric motors. Several types of tight lid for bearings made from Carbon Steel plates were obtained. Due to the elastic proprieties of the circular edge of the part obtained using this deformation method, this tight lid is used in the same time as safety Seger ring for the bearings.

In the last years, this new plastic deformation method was improved to obtain spherical segment shaped plates made from porous materials, specially designed to protect the molecular sieves in the air filtration and drying modules (components of pressure swing adsorption oxygen generator systems) [5,6,7,9].

In principle, the new plastic deformation process using pressured gazes blasting and impact substances, is based on the physical phenomenon of compressed gas discharged from a pressured vessel.

A special convergent-divergent nozzle was designed to obtain 350÷720m/s discharge velocity. The pressured gaze's shock wave combines the impact substances (pulverulent / fluid), which are

accelerated to the circular plate embedded in the contour of an open die. A plastically deformed part is obtained *with no punch die action* [5,7, 9].

In order to estimate the performance of this new plastic deformation process, an experimental research method was designed for simultaneous determination of the maximum transverse deformation, and of the deformation velocity of the thin plate deformed by gazes blasting shocks combined with different quantities of impact substances (quartz; water).

## 2. Theoretical considerations concerning the blasting shock wave velocity

Technical equipment functioning, usually called air cannon /air blaster, is based on the expanding effect of the compressed gas wave shock discharged with high velocity from a storage vessel.

During this fast process, the gas flow is characterized by high rate pressure variation; therefore there is no heat exchange with the outside environment, and the flow process can be considered adiabatic.[5,7]

For adiabatic process, from the Bernoulli equation for compressible fluids, it results:

$$\frac{v^2}{2} + \frac{k}{k-1} \cdot \frac{p}{\rho} = \frac{v_o^2}{2} + \frac{k}{k-1} \cdot \frac{p_o}{\rho_o}, \quad (1)$$

where  $p_o$  and  $\rho_o$  are the initial parameter of the gas;  $p$  and  $\rho$  are the final parameter of the gas;  $k$  is the adiabatic coefficient;  $v_o$  is the initial gas velocity (in the storage vessel  $v_o=0$ ).

In contrast with slow / static adiabatic transformations, which are isentropic (the entropy  $S$  is constant), the dynamic adiabatic transformations are irreversible (it take place with entropy increasing due to the internal heat stored in gas due to viscosity forces).

Neglecting the viscosity force, this motion can be considered an isentropic one, this hypothesis being admissible for gas blaster discharge phenomena.

When the compressed gas is discharging from a storing vessel (initial parameter  $p_o, \rho_o, T_o$ ) through a nozzle in the atmosphere (characterized by parameter  $p_{at}, \rho_{at}, T_{at}$ ), the gas velocity is determined with relation:

$$v = \frac{2k}{k-1} \cdot \sqrt{\frac{\rho}{\rho_o} \cdot \left[ 1 - \left( \frac{p_{at}}{p_o} \right)^{\frac{k-1}{k}} \right]} \quad (2)$$

Considering the initial parameter and the final parameter of the gas ( $k = 1,4$ ;  $p_o = 5-25$  bar;  $p_{at} = 1$  bar;  $T_o = T_{at} = 293$  °K), the velocity of the pressured air discharged from the storing vessel is presented in Table 1.

**Table 1**

$p_o$ [bar]	<b>5</b>	<b>6</b>	<b>7</b>
$\rho$ [kg/m <sup>3</sup> ]	5,946	7,135	8,324
$v$ [m/s]	465,8	485,6	501
$p_o$ [bar]	<b>8</b>	<b>9</b>	<b>10</b>
$\rho$ [kg/m <sup>3</sup> ]	9,522	10,713	11,903
$v$ [m/s]	513,2	523,6	532,4
$p_o$ [bar]	<b>15</b>	<b>20</b>	<b>25</b>
$\rho$ [kg/m <sup>3</sup> ]	16,564	22,327	28,778
$v$ [m/s]	584,6	623,8	687,5

Using the same method is possible to obtain  $\rho$  and  $v$  values for different initial pressured nitrogen.

The theoretical considerations concerning the gas discharge from the stocking vessel take into account the similitude with the flow process into round free jet.

Qualitative and quantitative evaluation of characteristic dimensions of the round free jet permit to determine the main manufacturing dimensional parameters of convergent - divergent nozzle which is able to direction the compressed gas shock wave to the embedded plate :  $b$  - distance from the jet pole;  $x_o$ -length of initial zone;  $\alpha$ -angle of jet action (Fig.1).

This free jet is a gas current that freely penetrates (with small friction forces to conical wall restriction) into an environment of the same or different gas (the

flow in jet is generally turbulent, particles of the discharged gas getting out its limits, with neighboring gas particles taking their place; a mass gas transfer with the exterior is achieved).

The jet's range is the distance where the kinetic energy of gas is not greater then the viscosity forces and therefore no more swirling flow appears.

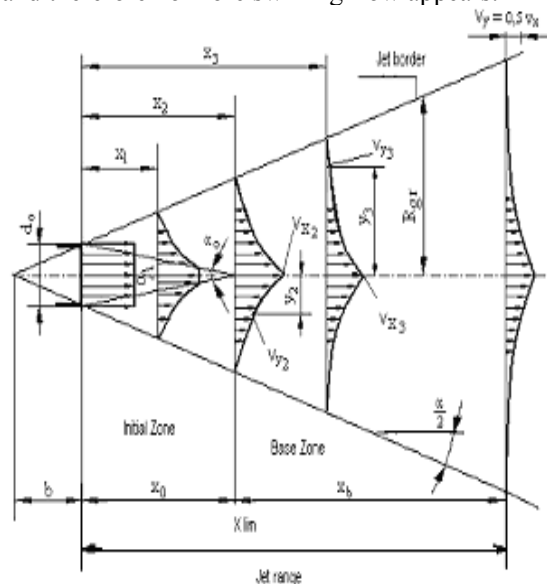


**Fig. 1**

The characteristic dimensions of a jet circular are: initial velocity  $v_o$ ; shape of the discharge nozzle; length of the initial zone  $x_o$ ; jet range  $x_{lim}$ ; convergence angle of the initial zone  $\alpha_o$ ; the enlarging jet border angle  $\alpha$ ; gas debit in initial section  $Q_o$ ; jet pole  $b$ ; jet radius  $R_{gr}$ .

The initial section of the discharging nozzle is the circular section in which the medium velocity  $v_o$  of the jet is realized. The environment velocity  $v_e$  can be equal to zero, bigger or smaller than  $v_o$  and for  $v_e = 0$ , the jet is considered to be free.

The velocity in the jet's axe  $v_x$  depends by the initial velocity  $v_o$  and by the distance  $x$ . For  $x < x_o$ , the velocity  $v_x = v_o$ , and for  $x > x_o$  the velocity  $v_x$  depends of distance  $x$ . The velocity in the transversal jet section  $v_y$  is the velocity at distance  $x$  and at the level  $y$ , depends by the velocity  $v_x$  and level  $y$ .

Theoretical and experimental researches determine the relation:

$$v_y / v_o = \left[ 1 - (y / R_{gr})^{3/2} \right]^2, \quad (3)$$

where  $R_{gr}$  is the jet's radius limit for  $x > x_o$ .

Due to the symmetric axial jet law, the impulse has the same value in any section. Using the notation  $v_y$  the velocity in a certain point,  $I$  the impulse, and

$m_o$  the masse passing through the elementary surface  $dA$  from the jets section in the time unity, it obtained:

$$I = 2\pi \int_0^{R_{gr}} \rho v_y^2 y dy = \pi \rho_o v_o^2 R_o^2, \quad (4)$$

where the jet's radius limit  $R_{gr}$  is obtained with the relation:

$$R_{gr} = 3,3 R_o (v_o / v_x), \quad (5)$$

where  $R_o$  is the jet' source radius.

The medium velocity of jet  $v_m$  is determined knowing that the medium flowing velocity in a section  $A$  is obtaining from the continuity equation:

$$v_m = Q / A = Q / (\pi R_{gr}^2). \quad (6)$$

Because in the initial section the velocity value is obtained with the relation  $v_o = Q / A = Q / (\pi R_o^2)$ , with relation (4) is obtained

$$v_m / v_o = 0,2 (v_x / v_o) \quad (7)$$

Using the above presented relations, for initial storage pressure  $p_o$  in the vessel, were obtained results for the jet range  $x_{lim}$ , the conical jet border angle  $\alpha$ , the jet diameter  $D_{gr}$  for jet range  $x_{lim}$ , the medium velocity  $v_m$  in the jet transversal section.

### 3. Experimental considerations concerning the shock wave dynamic pressure

In principle, the experimental installation for plastic deformation by gazes blasting and impact substance (Fig. 2) consists in a compressed gaze's supply; a compressed gaze's stocking vessel with quick discharge device (SVDD); impact particles dozing system; a modular die device with adjustable hydraulic action; a modular conical convergent-divergent nozzle.[5,7,8]

The experimental installation for plastic deformation is connected with a complex data acquisition and processing system composed of pressure or displacement transducer; conditioning amplifier; measuring amplifier; acquisition interface (PCL Advantech) and computer [5,8 ].

In order to determine the dynamic pressure produce by the SVDD with stocking vessel  $0,050 \text{ m}^3$  was made an experimental device, in principle, consisting in a conical nozzle ( $\varnothing_{max} / \varnothing_{min} = 300/100$ ;  $h = 250$ ) closed at the large base with a rigid metallic round flange, respectively in direct connection with the circular nozzle of the quick discharge device.

The size and the dimension of the conical nozzle are designed according the presented relations given

for jet range  $x_{lim}$ , conical jet border angle  $\alpha$ , the jet diameter  $D_{gr}$  for jet range  $x_{lim}$ .

On the rigid metallic round flange were disposed three pressure transducer connected with an amplifier device to a data acquisition system, respectively an acceleration transducer connected with another amplifier device and data acquisition system.

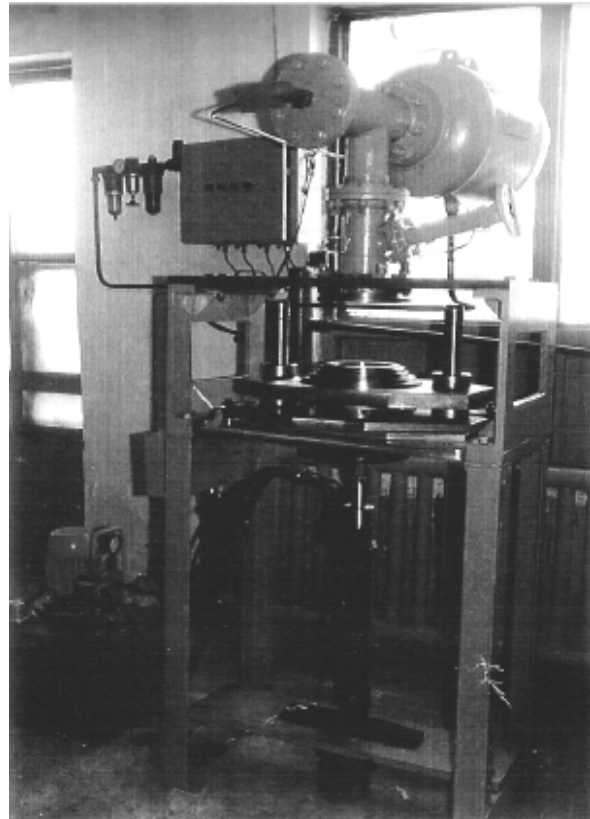


Fig. 2

The values obtained for the dynamic pressure  $p_{din}$ , the shock wave acceleration  $a_{sw}$  and the specific energy of the shock wave  $E_{sw}$ , determined for usual / high initial nitrogen pressure  $p_o$  in the stocking vessel are presented in Table 2.

Table 2

$p_o$ [bar]	$p_{din}$ [bar/s]	$a_{sw}$ [m/s <sup>2</sup> ]	$E_{sw}$ [J]
5	165,5	49,8	174,2
6	209,7	62,3	256,4
7	302,3	69,5	314,7
8	389,9	78,9	405,6
9	464,6	92,2	492,7
10	533,2	105,8	572,3
15	697,4	167,4	726,8
20	805,7	232,7	845,5
25	987,5	303,2	995,1

#### 4. Theoretical considerations concern large deformations of circular plate, produced by static load

In the simple bending of circular plate problem, the deformations in the middle plan of the plate can be neglected in the situation of small deformations in comparison with the plate thickness.[10]

The large deformations of circular plate solving problem must take in consideration all the deformations produced by bending efforts in the middle plan of the plate.

The circular plate deformations produced by bending moment uniform distributed on the circular contour of the plate, determine a symmetrical surface in rapport with the centre of the deformed plate. In this situation, the displacement of a point situated in the middle plan of the plate has two components: a component  $u$  in the radial direction, and a component  $w$  in the normal plan of the plate.

The radial deformation is obtained with relation

$$\varepsilon_r = \frac{du}{dr} + \frac{1}{2} \left[ \left( \frac{du}{dr} \right)^2 + \left( \frac{dw}{dr} \right)^2 \right] \quad (8)$$

and the tangential deformation is obtained with relation

$$\varepsilon_t = \frac{u}{r}, \quad (9)$$

where  $r$  represents the radius of the circular plate.

Noting the radial stress  $N_r$  and tangential stress  $N_t$  and applying the Hooke law, is obtained

$$N_r = \frac{Eh}{1-\nu^2} (\varepsilon_r + \nu \cdot \varepsilon_t) = \frac{Eh}{1-\nu^2} \left[ \frac{du}{dr} + \frac{1}{2} \left( \frac{dw}{dr} \right)^2 + \nu \frac{u}{r} \right] \quad (10)$$

$$N_t = \frac{Eh}{1-\nu^2} (\varepsilon_t + \nu \varepsilon_r) = \frac{Eh}{1-\nu^2} \left[ \frac{u}{r} + \nu \left( \frac{dw}{dr} \right)^2 + \nu \frac{du}{dr} \right]$$

These stresses must to be considered to determine the equilibrium equation in the plate element. The projection sum on the radial direction of all the forces stressing the considered element, determine the equation

$$N_r - N_t + r \frac{dN_r}{dr} = 0 \quad (11)$$

The relation (11) represents an approximate solution to determine the elastic-plastic deformation of the round plate embedded on circular contour, stressed by a uniform distributed pressure, that must

take in consideration the force  $Q_r$  action which is distributed on the tangential plan of each normal elementary surface.

The second equilibrium equation is obtained taking in consideration the moments determined by all the forces in rapport with a normal axe on the radius

$$Q_r = -D \left( \frac{d^3 w}{dr^3} + \frac{1}{r} \frac{d^2 w}{dr^2} - \frac{1}{r^2} \frac{dw}{dr} \right), \quad (12)$$

where  $D$  represents the bending rigidity of the plate.

The  $Q_r$  average take into consideration the equilibrium of a circular interior zone (circular zone with  $r$  radius), described by the relation

$$Q_r = -N_r \frac{dw}{dr} = -\frac{1}{r} \int_0^r p r dr \quad (13)$$

After introducing relation (13) in equation (12), and using the relations (10) for  $N_r$  and  $N_t$ , the equations (11) and (12) can be written as the following nonlinear equations

$$w_0 = \frac{pa^4}{64D} \left[ 1 + 0,146 \left( w_0^2 / h^2 \right) \right] \quad (14)$$

$$\frac{d^3 w}{dr^3} = -\frac{1}{r} \frac{d^2 w}{dr^2} + \frac{1}{r^2} \frac{dw}{dr} + \frac{12}{h^2} \frac{dw}{dr} \left[ \frac{du}{dr} + \nu \frac{u}{r} + \frac{1}{2} \left( \frac{dw}{dr} \right)^2 \right]$$

These nonlinear equations can be integrated starting from the centre of the plate, and increasing by small steps in radial direction.

For the central circular element is admitted a radial deformation given by the relation

$$\varepsilon_0 = \left( \frac{du}{dr} \right)_{r=0},$$

and a uniform curve radius given by the relation

$$\frac{1}{\rho_0} = - \left( \frac{d^2 w}{dr^2} \right)_{r=0}.$$

With these values of the radial deformation and of the uniform curve radius to the centre of the plate, the radial deformation values  $u$ , and the  $(dw/dr)$  values in each tangent on the deformation curve, can be determined. In this manner, all the quantities in the right side of the relation (14) are known, and the values for  $(d^2 u/dr^2)$  and  $(d^3 w/dr^3)$  can be determined for any value of the radius  $r$ .

This method can be used to determine the transversal stresses of the circular plate (radius  $a$ ) rigid embedded on the contour, stressed by a uniform distributed pressure. Due to this pressure, the deformation curve equation is supposed to be described by the relation

$$w = w_0 \left( 1 - \frac{r^2}{a^2} \right)^2, \quad (15)$$

where the deformation in the centre of the plate is determined with the cubic relation

$$w_0 = \frac{pa^4}{64D} \left[ 1 + 0,488 \left( w_0^2 / h^2 \right) \right] \quad (16)$$

The last factor in the right side of the equation (16) represents the effect of middle surface increasing on the total deformation of the plate.

Supposing that the embedded plate can have a radial boundary slipping, the deformation in the centre of the plate can be determined with the relation

$$w_0 = \frac{pa^4}{64D} \left[ 1 + 0,146 \left( w_0^2 / h^2 \right) \right] \quad (17)$$

Considering the general equations for radial and tangential deformations given by the relations (8), (9) and (10), it can be observed that if  $N_r = 0$  on the contour, then the value on the contour of  $N_t$  become a negative one ( $N_t = Eh\varepsilon_t = Ehu/r$ ).

This means that for transversal loads critical values, the boundary embedded contour might become instable (occurs the slipping of the plate in the embedded contour).

To prevent the slipping process on the embedded contour, Nadai proposed to determine the deformation in the centre of the plate using the following cubic relation in equation (14) [10]

An exact solution to determine *the large deformation of a circular plate embedded on the contour, and stressed by uniform distributed pressure*, is necessary to solve the equations

$$\frac{d^2u}{dr^2} + \frac{1}{r} \frac{du}{dr} - \frac{u}{r^2} = -\frac{1-\nu}{2r} \left( \frac{dw}{dr} \right)^2 - \frac{dw}{dr} \frac{d^2w}{dr^2} \quad (18)$$

$$\frac{d^3w}{dr^3} + \frac{1}{r} \frac{d^2w}{dr^2} - \frac{1}{r^2} \frac{dw}{dr} = \frac{12}{h^2} \frac{dw}{dr} \times \left[ \frac{du}{dr} + \nu \frac{u}{r} + \frac{1}{2} \left( \frac{dw}{dr} \right)^2 \right] + \frac{1}{Dr_0} \int_0^r pr \, dr$$

Nadai proposed to admit that the deformation of circular plate embedded on contour have to take in consideration in relations (18) the approximate relation [10]

$$\frac{dw}{dr} = C \left[ \frac{r}{a} - \left( \frac{r}{a} \right)^n \right] \quad (19)$$

which become zero for  $r = 0$  and  $r = a$ , in correlation with the conditions of the circular plate embedded on the contour.

The first of equation (18) solve the approximate value for  $u$ . Introducing these approximations for  $u$  and  $dw/dr$  in the second equation (18), the relation

to determine the deformation in the centre of the circular plate is given by the relation

$$\frac{w_0}{h} + 0,583 \left( \frac{w_0}{h} \right)^3 \approx 0,176 \frac{P}{E} \left( \frac{a}{h} \right)^4 \quad (20)$$

The first rapport in the left side of previous equation can be neglected (due to very small value in comparison with the second), and the deformation can be determined with relation

$$0,583 \left( \frac{w_0}{h} \right)^3 \approx 0,176 \frac{P}{E} \left( \frac{a}{h} \right)^4 \quad (21)$$

This relation show that the deformation is not proportional with the load intensity, but depends with the  $p^{1/3}$  increasing.

The exact solution of the large deformations problem can by obtained taking in consideration that in the equations (18), the first one of these equations is equivalent to equation (11).

Taking in consideration the relation (13), the second equation (18) can be written as the following relation

$$D \left( \frac{d^3w}{dr^3} + \frac{1}{r} \frac{d^2w}{dr^2} - \frac{1}{r^2} \frac{dw}{dr} \right) = N_r \frac{dw}{dr} + \frac{pr}{2} \quad (22)$$

Considering the general relations for radial and tangential deformations, we obtain the relation

$$\varepsilon_r = \varepsilon_t + r \frac{d\varepsilon_t}{dr} + \frac{1}{2} \left( \frac{dw}{dr} \right)^2 \quad (23)$$

Introducing notations

$$\varepsilon_r = \frac{1}{Eh} (N_r - \nu N_t) \quad (24)$$

and

$$\varepsilon_t = \frac{1}{Eh} (N_t - \nu N_r) \quad (25)$$

in these equations, and using the relation (11), we can obtain the equation to determine the deformation in the centre of the circular plate

$$r \frac{d}{dr} (N_r + N_t) + \frac{Eh}{2} \left( \frac{dw}{dr} \right)^2 = 0 \quad (26)$$

These theoretical considerations permit to determine the deformation in the centre of the embedded circular plate, using the relation

$$\frac{w_0}{h} + A \left( \frac{w_0}{h} \right)^3 = B \frac{P}{E} \left( \frac{a}{h} \right)^4 \quad (27)$$

The radial tensile and the tangential tensile *in the middle plan* of the circular plate can be determined using the relations

$$\sigma_{rad,mp} = \alpha_{rad} E \left( \frac{w_0}{a} \right)^2 \quad (28)$$

$$\sigma_{tg,mp} = \alpha_{tg} E \left( \frac{w_0}{a} \right)^2 \quad (29)$$

The radial tensile and the tangential tensile *in the extreme fiber* of the circular plate can be determined using the relations

$$\sigma_{rad,ef} = \beta_{rad} E \frac{w_0 h}{a^2} \quad (30)$$

$$\sigma_{tg,ef} = \beta_{tg} E \frac{w_0 h}{a^2} \quad (31)$$

The coefficients in relations (27),..., (31), are [10]:

- Rigid boundary  $A = 0,47; B = 0,17$
- in the centre  $\alpha_{rad} = \alpha_{tg} = 0,97$  ;  
 $\beta_{rad} = \beta_{tg} = 2,86$
- on the boundary  $\alpha_{rad} = 0,47; \alpha_{tg} = 0,14$   
 $\beta_{rad} = -4,4; \beta_{tg} = -1,32$
- Mobil boundary  $A = 0,14; B = 0,17$
- in the centre  $\alpha_{rad} = \alpha_{tg} = 0,5$  ;  
 $\beta_{rad} = \beta_{tg} = 2,86$
- on the boundary  $\alpha_{rad} = 0; \alpha_{tg} = -0,33$   
 $\beta_{rad} = -4,4; \beta_{tg} = -1,32$ .

Using this method, the deformations  $w_0$  in the centre of the circular embedded plate ( $h = 1 \text{ mm}$ ;  $a = 130 \text{ mm}$ ) made in AISI 316 stainless steel, produced by static pressure, are presented in Table 3.

**Table 3**

$p$ [bar]	$w_0$ [mm]	$p$ [bar]	$w_0$ [mm]
10	10,8	60	22,3
20	14,7	70	23,8
30	17,3	80	25,1
40	19,6	90	26,2
50	21,2	100	27,4

To obtain spherical shaped the static pressure can be uniform distributed utilizing an elastic membrane made in very resistant material on the hydrostatic action; but this elastic membrane can not be used when the necessary to be deformed is punched.[2]

To evaluate the deformability of the plate with  $w_{pl,max} = 22...25\text{mm}$  depth deformation, plastic deformed considering a rigid embedded boundary, the radial stress and the tangential stress were determined (Table 4).

In order to compare the theoretical method results, an analytical method based on the finite element method (FEM) was used [4].

In Table 4 is observed that the values obtained using FEM are 4...10% smaller then the values obtained using the presented theoretical method (AM).

**Table 4**

Fibre position [mm]	Tangential stress $\sigma_{tg}$ [N/mm <sup>2</sup> ]		Radial stress $\sigma_{rad}$ [N/mm <sup>2</sup> ]	
	AM	FEM	AM	FEM
Internal $z = 0,5$	155	147	203	191
Central $z = 0$	-22	-19	42	39
External $z = -0,5$	-103	-96	-121	-112

## 5. Theoretical considerations concern large deformations of circular plate, produced by impulsive load

Starting from the theoretical studies for impulsive loads deformation processes, it was developed a mathematical method for plastic deformation by gas blasting combined with impact quantities.

This model is based on the hypothesis theory which takes into account that the external forces deformation energy is consumed to exceed the bending strain energy and the stretch strain energy plate deformation energy, described by Lagrange equation: [1,5]

$$\int (\Delta W_{ext} + \Delta W_{cin}) - \int \Delta W_p = 0 \quad (32)$$

The external forces energy variation is achieved due to the direct shock wave action produced by the gas blasting combined with the impact substance effect

$$\Delta W_{ext} = \frac{1}{\rho_0 \cdot c_0} \int_0^{t_m} p_{(t)}^2 \cdot dt = \frac{1}{\rho_0 \cdot c_0} \int_0^{t_m} (p_{max} \cdot e^{-t/\theta})^2 \cdot dt \quad (33)$$

where  $t_m$  is the moment when is achieved the maximum wave pressure  $p_{max}$  on the deformed plate.

The kinetic energy variation could be described with relation:

$$\Delta W_{cin} = \frac{\rho_m}{2} \int \left[ \left( \frac{\partial w}{\partial t} \right)^2 + \left( \frac{\partial u}{\partial t} \right)^2 \right] \cdot dV_m \quad (34)$$

where  $\rho_m$  and  $V_m$  represent the density and the volume of the deformed material;  $w = w(r; t)$  represent the depth of the deformation;  $u = u(r; t)$  represent the radial displacement.

The potential energy variation could be described with the relation:

$$\Delta W_{pot} = \int (\sigma_{rad} \cdot \Delta \varepsilon_{rad} + \sigma_{cf} \cdot \Delta \varepsilon_{cf}) \cdot dV_m \quad (35)$$

where  $\sigma_{rad}$  and  $\varepsilon_r$  represent the radial tensile stress, and the radial deformation, respectively;  $\sigma_{cf}$  and  $\varepsilon_{cf}$  represent the circumferential tensile stress, and the circumferential deformation, respectively.

The relations between tensile stresses are based on the following hypothesis: the deformation of the material' volume is proportional with the medium normal tensile; the value of the tensile depends on the deformation value; the deviator functions of tensile are proportional with the deformations.

In hypothesis that the external forces are consumed by the resistance forces such as bending strain forces and the stretch strain forces, the specific radial and circumference deformation which are placed in the medium plane  $z$ , could be calculated with relations

$$\varepsilon_r = \frac{\partial u}{\partial r} + \frac{1}{2} \left( \frac{\partial w}{\partial r} \right)^2 - z \cdot \frac{\partial^2 w}{\partial r^2} \quad (36)$$

$$\varepsilon_{cf} = \frac{u}{r} - \frac{z}{r} \frac{\partial w}{\partial r} \quad (37)$$

Corresponding with these deformations, the tensile are calculated with the relations [10]

$$\sigma_r = \frac{I}{I - \nu^2} \cdot \frac{\sigma_{ech}}{\varepsilon_{ech}} (\varepsilon_r + \nu \cdot \varepsilon_{cf}) \quad (38)$$

$$\sigma_{cf} = \frac{I}{I - \nu^2} \cdot \frac{\sigma_{ech}}{\varepsilon_{ech}} (\varepsilon_{cf} + \nu \cdot \varepsilon_r), \quad (39)$$

where:

$$\sigma_{ech} = \left( \sigma_r^2 + \sigma_r \cdot \sigma_{cf} + \sigma_{cf}^2 \right)^{1/2} \quad (40)$$

$$\varepsilon_{ech} = \frac{I}{I - \nu^2} \left[ \left( \varepsilon_r^2 + \varepsilon_{cf}^2 \right) \left( \nu^2 - \nu + I \right)^{1/2} - \right. \quad (41)$$

$$\left. - \frac{I}{I - \nu^2} \left[ \varepsilon_r \cdot \varepsilon_{cf} \left( \nu^2 - 4\nu + I \right) \right]^{1/2} \right]$$

In the dynamic elastic deformation, the material is deformed according Hooke law, given by relation:

$$\sigma_{ech} = E_d \cdot \varepsilon_{ech}, \quad (42)$$

where  $E_d$  is the dynamic elasticity modulus (presumed to be equal with the static one)[2,5].

In the plastic deformation range, the material is deformed according the relation:

$$\sigma_i = E_d \cdot \varepsilon_i \left( 1 - f(\varepsilon_i) \right) \quad (43)$$

where  $f(\varepsilon_i)$  depends on cold-hardening characteristic, which is calculated for linear hardening with the relation:

$$f(\varepsilon_i) = \frac{\varepsilon_i - \varepsilon_c}{\varepsilon_i} \cdot f \quad (44)$$

where  $\varepsilon_c$  represents the relative deformation corresponding to yield point;  $\varepsilon_i$  represents the depth of the deformation  $w$ , and circumference deformation  $r$ , respectively;  $f_E$  represents the coefficient depending on elasticity material modulus:

$$f_E = \frac{E_d - E_p}{E_d} \quad (45)$$

The deformation velocity is calculated with the relation

$$\dot{\varepsilon} = \frac{\partial \varepsilon_i}{\partial t}, \quad (46)$$

where  $n$  represents the cold-hardening coefficient;  $K$  represents the dynamic tensile strength (experimentally determined for each impulsive deformed material).

Notation  $\sigma_r^m, \sigma_{cf}^m$  and  $\varepsilon_r^m, \varepsilon_{cf}^m$  the tensile and the deformations at the moment  $t_m$ , which correspond with the direct shock wave stopping action, after this moment the tensile and the deformations can be calculated with relation:

$$\sigma_r = \sigma_r^m \frac{I}{I - \nu^2} \left[ \left( \varepsilon_r^m + \nu \cdot \varepsilon_{cf}^m \right) - \left( \varepsilon_r + \nu \cdot \varepsilon_{cf} \right) \right] \quad (47)$$

$$\sigma_{cf} = \sigma_{cf}^m \frac{I}{I - \nu^2} \left[ \left( \varepsilon_{cf}^m + \nu \cdot \varepsilon_r^m \right) - \left( \varepsilon_{cf} + \nu \cdot \varepsilon_r \right) \right] \quad (48)$$

To establish the deformation values and the tensile values in each point of the deformed material, for every moment of the deformation process, it can be given an equation system, using the following notations:

$$r_l = \frac{r}{R}; z_l = \frac{z}{h}; w_l = \frac{w}{h}; h_l = \frac{R}{h}; n^2 = h^2 \frac{u}{R}.$$

Taking into account the limit conditions considered for the material which is embedded on circular form, given by the relations:

$$w_l(r, t) = 0; \frac{\partial w_l}{\partial r_l} = 0; n(r_l; t) = 0 \quad (49)$$

the results could be written as relations (50):

$$w_l(r, t) = \sum_{i=1}^k a_i(r_l) \cdot w_{li}; n(r_l; t) = \sum_{j=1}^m b_j(r_l) \cdot c_j(t) \quad (50)$$

Replacing relations (50) in relations (37) and (36), we obtain the equation system (51) and (52):

$$\Delta \varepsilon_r = h^2 \left\{ \sum_{j=1}^m c_j(t) \cdot \frac{\partial (b_j(r_l))}{\partial r_l} + \frac{1}{2} \left[ \sum_{j=1}^k w_j(t) \cdot \frac{\partial (a_j(r_l))}{\partial r_l} \right]^2 \right\} - \quad (51)$$

$$- h^2 z_l \frac{\partial^2}{\partial r_l^2} \left[ \sum_{j=1}^k w_j(t) \cdot a_j(r_l) \right]$$

$$\Delta \varepsilon_{cf} = h^2 \left[ \frac{1}{r_l} \sum_{j=1}^m c_j(t) \cdot b_j(r_l) - \frac{z_l}{r_l} \sum_{j=1}^k w_j(t) \cdot \frac{\partial (a_j(r_l))}{\partial r_l} \right] \quad (52)$$

Replacing relations (51) and (52) in relation (35), and then in relation (1), where ( $i = 1, k$  and  $j = 1, m$ ), we obtain a differential equations system (53):

$$\begin{aligned}
 & b_l \sum_{i=1}^k \ddot{f}(\varepsilon_i) \int_{-1/2}^{+1/2} \int_0^1 a_i a_i(r_i) r_i d r_i d z_i = \\
 & -2c_l \sum_{i=1}^k f(\varepsilon_i) \int_{-1/2}^{+1/2} \int_0^1 \varepsilon_i a_i(r_i) \cdot \frac{\partial}{\partial r_i} a_i(r_i) r_i d r_i d z_i + \rho_w \int_0^1 a_i(r_i) \cdot r_i d r_i \\
 & + 2c_l \int_{-1/2}^{+1/2} \int_0^1 \left( z_l \frac{\partial^2}{\partial r_i^2} a_i(r_i) \varepsilon_i r_i + \frac{z_l}{r_i} \cdot \frac{\partial}{\partial r_i} a_i(r_i) \varepsilon_i r_i \right) r_i d r_i d z_i
 \end{aligned}
 \tag{53}$$

$$\begin{aligned}
 & b_l \sum_{i=1}^k \ddot{f}(\varepsilon_i) \int_{-1/2}^{+1/2} \int_0^1 a_i a_i(r_i) r_i d r_i d z_i = \\
 & -2c_l \sum_{i=1}^k f(\varepsilon_i) \int_{-1/2}^{+1/2} \int_0^1 \varepsilon_i a_i(r_i) \cdot \frac{\partial}{\partial r_i} a_i(r_i) r_i d r_i d z_i + \rho_w \int_0^1 a_i(r_i) \cdot r_i d r_i \\
 & + 2c_l \int_{-1/2}^{+1/2} \int_0^1 \left( z_l \frac{\partial^2}{\partial r_i^2} a_i(r_i) \varepsilon_i r_i + \frac{z_l}{r_i} \cdot \frac{\partial}{\partial r_i} a_i(r_i) \varepsilon_i r_i \right) r_i d r_i d z_i
 \end{aligned}$$

Substituting  $\sigma_r$  and  $\sigma_{cf}$  in previous relations, it must be taken account that for each step of integration, it is necessary to control if the deformation process is elastic, or a plastic one.

The equations system (24) and (25) can be solved utilizing Runge-Kutta method, and permit to establish the radial and the circumferential tensile ( $\sigma_r$ ;  $\sigma_{cf}$ ) for each point of material thickness and for every range of stress deformations.

In order to compare the experimental results, an analytical method based on the finite element method (FEM) was used [4]. In Table 5 is observed that the values obtained using FEM are 3...7% smaller then the values obtained using the presented analytical method (AM).

**Table 5**

Fibre position [mm]	Circumferential stress $\sigma_{cf}$ [N/mm <sup>2</sup> ]		Radial stress $\sigma_{rad}$ [N/mm <sup>2</sup> ]	
	AM	FEM	AM	FEM
Internal $z = 0,5$	183	174	244	232
Central $z = 0$	-33	-29	54	48
External $z = -0,5$	-126	-117	-145	-136

## 6. Experimental considerations concerning the deformation depth / velocity

In order to determine the maximum transverse deformation, the permanent transverse deformation respectively, the mobile part of 3 displacement transducers were mounted in the control node 1N, 11N and 21N of the circular plate part (Fig. 3).[5]

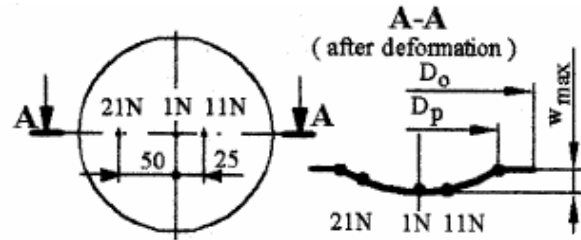


**Fig. 3**

The deformation velocity was analytically determined by means of the acquisition and processing data system for each value of initial representative pressure  $p_0$  inlet the stocking vessel.

For each parameter combinations between deformable circular plate / initial pressure  $p_0$  in the stocking vessel / quantity of impact particles, at the acquisition start command, it was used a triggering signal, from the control coil of the electro-pneumatic valve (due to the controlled supersonic gazes discharge is obtained).

The maximum transverse deformation velocity in each control node was analytically calculated and graphically represented by means of the data acquisition and processing system, for each initial representative pressure  $p_0$  for which the porous material has significant deformations.

Spherical segment shaped plates with circular punches achieved respecting the technologically parameter described in this paper, are made for a filtration equipment to obtain different concentrated fruit juice.

For the experiments described in this paper there were used circular discs made on AISI 316 stainless steel (1 mm thickness;  $D_0 = 130$  mm;  $\Phi 0,8$  punch; 40 punches/cm<sup>2</sup>). According to the filtration stage where is necessary to be mounted, the spherical segment shaped plates plastic deformed by this method, must have the final dimensions  $D_p = 110$  mm,  $w_{pl, max} = 22...25$  mm.

To avoid energy losses due to the round punches in the material, each circular part is covered on both sides with very thin plastic material (PVC).

In order to compare the experimental results, an analytical method based on the finite element method (FEM) was used.

FEM takes into account the following hypothesis: the large specific deformations must consider the isotropic hardening of the material; the deformable thin plate is considered as PLANE 2D axial-symmetrical elements, with GAP contact element with no friction.

In the dynamic nonlinear analysis, for a quick convergence, the Newton - Raphson method was used and, as an integration method, the Newmark method with Rayleigh amortization factor for

maximum 0,4s time range, divided in an increment  $DT_{min} = 1E-6$  and  $DT_{max} = 5E-4$  [4].

The synthetic comparison between the maximum transverse deformation velocity values, on the plastically deformed stainless steel part obtained using only pressured nitrogen blasting shock wave produced by initial pressure  $p_0 = 10\text{bar}$ , experimentally determined with Hottinger transducers placed on three nodes of the round disc, and the analytically obtained values with FEM, is presented in Table 6.

**Tabel 6**

Maximum transverse deformation velocities in control nodes of the disc, [m/s] (control radius, [mm])				
1N (0)	11N (25)	21N (50)	31N (55)	41N (60)
<b>Experimental Method</b>				
1,7	1,5	1,3	-	-
<b>Analytical Method (FEM)</b>				
1,62	1,41	1,22	1,16	1,02

In Table 6 can be observed that the values obtained using FEM are 6...8% smaller then the values determined using experimental method.

The maximum transverse elastic deformation and the transverse plastic deformation in control nodes of the deformed plate, obtained using only nitrogen blasting shock wave produced by the consecutive increasing of the initial pressure  $p_0$  from 7,5 bar to 25 bar, are presented in Table 7. The experimental method concerned in three transducers placed on three control nodes of the plate (1N; 11N; 21N).

**Table 7**

$p_0$ [bar]	$w_{el,max}$ [mm]	Transverse plastic deformation in control nodes of the plate (control radius, [mm])		
		1N (0)	11N (25)	21N (50)
7,5	8,3	6,2	5,8	5,5
8	9,2	7,3	6,8	6,4
8,5	10,1	8,1	7,7	7,2
9	10,8	8,9	8,6	8,2
9,5	11,7	9,8	9,5	9,2
10	12,2	10,2	9,9	9,5
15	16,7	14,5	12,4	11,3
20	21,3	19,8	18,1	16,5
25	26,8	24,7	23,5	21,6

In Table 7 is observed that only using an initial nitrogen pressure  $p_0 = 25$  bar is possible to be obtained plastic deformation depth more then 22 mm.

The maximum transverse elastic deformation and the transverse plastic deformation in control nodes 1N; 11N; 21N of the deformed plate,

produced only by nitrogen blasting shock wave produced by the consecutive increasing of the initial pressure  $p_0$  from 9bar to 40bar, obtained using FEM, are presented in Table 8.

Comparing the values presented in Table 7 and Table 8 can be observed that the FEM values are 5...10 % smaller then the values determined by experimental method.

In Table 8 can be observed that using only initial pressure larger then 25 bar is possible to obtain plastic deformed plate with 22,8...32,2mm central depth deformation.

**Table 8**

$p_0$ [bar]	$w_{el,max}$ [mm]	FEM plastic deformation in control nodes of the plate (control radius, [mm])		
		1N (0)	11N (25)	21N (50)
9	10,2	8,1	7,5	6,8
9,5	11,1	9,2	8,7	8,1
10	12,5	11,7	10,9	9,8
15	15,3	13,8	11,7	10,9
20	19,4	18,4	17,1	16,0
25	24,6	22,8	21,2	20,1
30	27,4	26,2	24,8	23,6
35	30,2	28,5	27,3	26,4
40	33,5	32,2	30,9	29,5

In Fig.4 is presented the FEM for maximum elastic deformation  $w_{el,max}$  for the transverse plastic deformation in control nodes of the plate, using initial nitrogen pressure 9,5 bar.

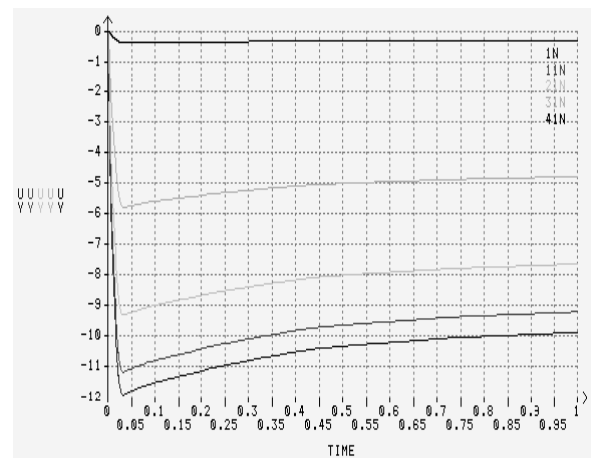


**Fig. 4**

The representative experimental data for transverse plastic deformation in 1N, 11N, 21N control nodes of the disc, obtained using initial nitrogen pressure 9,5 bar are presented in Fig. 5.

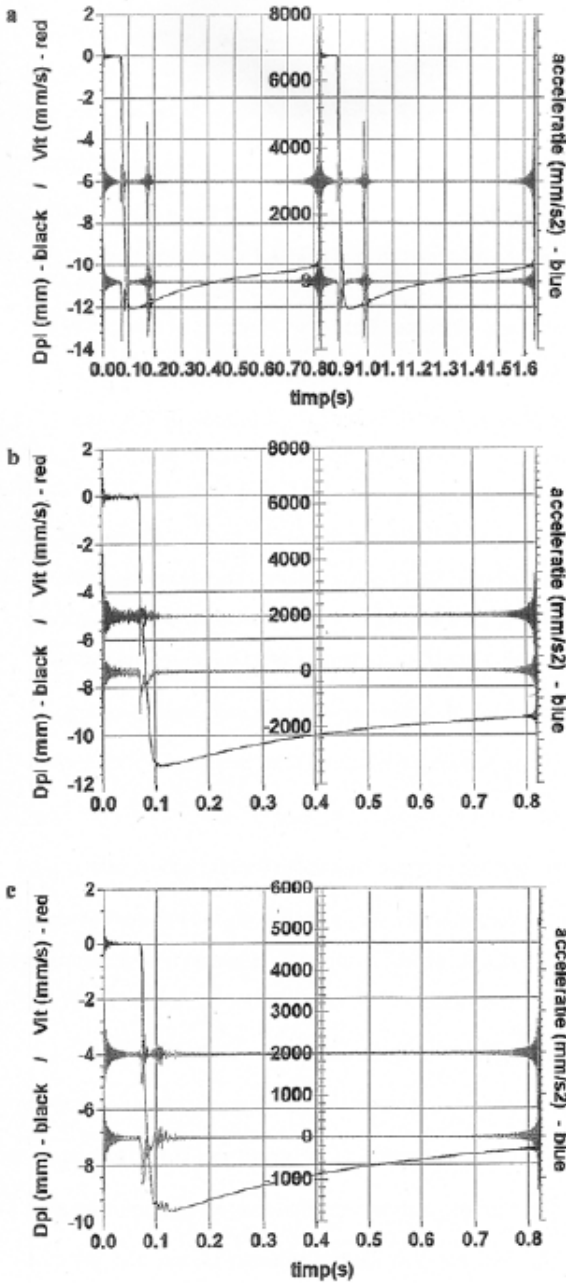


Fig. 5

In order to increase the depth of the plastic deformed part, it was necessary to increase the kinetically energy of the shock wave by introducing impact substance in combination with the nitrogen blasting shock wave.

To make spherical segment plates with small punches, plastic deformed at more then 22mm maximum depth, as impact substance were used several quantities of water (1dm<sup>3</sup>; 1,5dm<sup>3</sup>; 2dm<sup>3</sup>) accelerated by increasing initial nitrogen pressure  $p_o = 7,5...25\text{bar}$ .

In Table 9 is presented the maximum deformation depth in the center of the plastic deformed plate using 1dm<sup>3</sup>; 1,5dm<sup>3</sup>; 2dm<sup>3</sup> water impact substances accelerated by initial nitrogen pressure  $p_o = 7,5...10\text{bar}$  (experimental method).

Table 9

Initial pressure inlet stocking vessel, [bar]					
7,5	8,0	8,5	9,0	9,5	10
Maximum deformation in the center of the plastic deformed plate, [mm]					
Nitrogen blasting shock wave combined with 1,0dm <sup>3</sup> water impact substance					
8,8	9,7	10,6	11,5	12,3	12,8
Nitrogen blasting shock wave combined with 1,5dm <sup>3</sup> water impact substance					
9,4	10,5	11,4	12,4	13,0	13,7
Nitrogen blasting shock wave combined with 2dm <sup>3</sup> water impact substance					
10,3	11,1	12,2	13,3	14,1	15,2

In Table 9 it can be observed that using an increasing quantity of water impact substance, it is possible to obtain larger values for the maximum depth (~ 25% for 1,0 dm<sup>3</sup> water impact substance; ~ 40% for 1,5 dm<sup>3</sup> water impact substance; ~ 50% for 2,0 dm<sup>3</sup> water impact substance) compared with the results obtained using only nitrogen blasting shock wave. It can be also observed that using these combinations is not possible to obtain plastic with more then 15,2mm depth deformation.

Fig. 6 presents the FEM results obtained for nitrogen initial pressure  $p_o=10\text{bar}$  shock wave combined with 1,5 dm<sup>3</sup> water impact substance.

The FEM values are 4-9 % smaller then the values determined using experimental method.

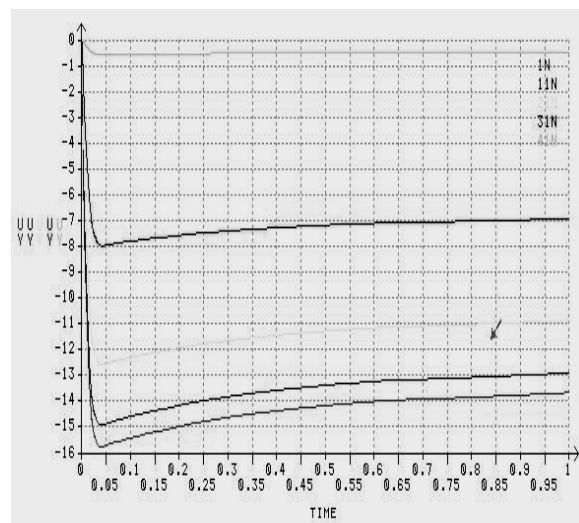


Fig. 6

In Table 10 is presented the maximum deformation depth in the center of the plastic deformed plate using 1dm<sup>3</sup>; 1,5dm<sup>3</sup>; 2dm<sup>3</sup> water impact substances accelerated by initial nitrogen pressure  $p_o = 15; 20; 25\text{bar}$  (experimental method).

**Table 10**

<b>Initial pressure inlet stocking vessel, [bar]</b>		
15	20	25
<b>Maximum deformation in the center of the plastic deformed plate, [mm]</b>		
<b>Nitrogen blasting shock wave combined with 1,0dm<sup>3</sup> water impact substance</b>		
16,2	18,6	22,3
<b>Nitrogen blasting shock wave combined with 1,5dm<sup>3</sup> water impact substance</b>		
19,8	22,8	25,7
<b>Nitrogen blasting shock wave combined with 2dm<sup>3</sup> water impact substance</b>		
22,4	24,3	28,1

In Table 10 is observed that using high nitrogen pressure combined with water impact substance is possible to obtain stainless steel spherical segment shape with final central depth deformation larger then the technological imposed value 22mm.

## 7. Conclusion

In the new high velocity deformation method presented in this paper, the contribution of the impact substances energy can be found both in the kinetic energy of the deformable plate, joined at a given moment (for a quantum time) with the mass of the impact substance, and in the same time, in the maximum dynamic pressure which interacts with the plate in the same quantum time.

Using usual initial nitrogen pressure  $p_o = 7,5 \dots 10\text{bar}$ , combined with 1dm<sup>3</sup>; 1,5dm<sup>3</sup>; 2dm<sup>3</sup> water impact substances is possible to obtain 15,2mm maximum deformation depth for stainless steel spherical segment shaped.

Using high initial nitrogen pressure  $p_o = 15; 20; 25\text{bar}$  combined with 1dm<sup>3</sup>; 1,5dm<sup>3</sup>; 2dm<sup>3</sup> water impact substance is possible to obtain stainless steel spherical segment shaped with final depth deformation larger then the technological imposed value 22mm.

The experimental research works show that the elastic maximal deformation is achieved in  $0,03 \div 0,06\text{sec}$  and the permanent plastic deformation is achieved in  $0,2 \div 0,4\text{sec}$ . Due to the velocity values is confirmed that the new method is a high velocity deformation method.

The deformation energy which characterizes this new plastic deformation method shows that the

efficiency of the plastic deformation process by gas blasting shock wave and impact substances is comparable with the efficiency of the classical high velocity deformation methods, such as deformation by explosive powders, deformation by electromagnetic impulses, and deformation by exploding wires in gas.

### References:

- [1] Cristescu, N., *Dynamic Plasticity*, North Holland Publishing Company, Amsterdam, 1987.
- [2] Ghizdavu, V., *Metals Processing by High Power and Velocities*, Technical Publishing House, Bucharest.
- [3] Muttelman, L.D., et al., *High Velocity Metals Deformation*. Mashinostroenie, Moscova.
- [4] Năstăsescu, V., *Finite Element Method*. Military Technical Academy Publishing, Bucharest, 2004
- [5] Roșca, A., *Contributions on Thin Sheets Deformed by Pneumatic Impulses and Impact Particles*, Ph. D. Thesis, University of Craiova, 1998.
- [6] Roșca, A., Roșca D., *Deformation Velocity of Thin Sheets Porous Materials Deformed by Air Blasting*, European Congress on Powder Metallurgy, PM 2001, vol.4, Nice, France, ISBN 1 899072-08 X, pp 258-261, 2001
- [7] Roșca, A., *Metals Deformability Deformed by Pneumatically Shock Waves*, ICMET Craiova Publishing House, ISBN 973-85113-1-3, 2001.
- [8] Roșca, A., Roșca, D., Năstăsescu, V., *Contributions on Pressured Gases Blasting in Applied Technologies*. Advanced Technologies Research – Development – Applications. Advanced Robotic System International, 2006, Pro Literatur Verlag, Mammendorf, Germany, ISBN 3-86611-197-5.
- [9] Roșca, A., *Shock wave pneumatic device*, Romanian Industrial Model, 1997.
- [10] Timoshenko, S.P., *Theory of Plates and Shells*, McGraw - Hill Book Company